Supporting Information to:

A comparison of zwitterionic and anionic mechanisms in the dual-catalytic polymerization of lactide

Alexander Balint[a] and Stefan Naumann*[a]

[a]Universtiy of Stuttgart, Institute for Polymer Chemistry, 70569 Stuttgart, Germany

Email: stefan.naumann@ipoc.uni-stuttgart.de

Table of Content

Experimental

Starting Materials and Catalyst Synthesis

L-Lactide (*L*-LA, TCI Chemicals) and *rac*-Lactide (*rac*-LA, TCI Chemicals) were dissolved in dry methylene chloride and stored over molecular sieve (3 Å) for two days. The solution was filtered, dried under vacuum and recrystallized from toluene (twice). The resulting crystalline precipitate was stored under protective conditions inside the glove box (LabMaster, *MBraun*, Germany, RT). Benzyl alcohol (BnOH, Sigma-Aldrich, 99.8 %) was dried over CaH_2 and subsequently distilled under static vacuum ($1 \cdot 10^{-3}$ mbar). The clear liquid was degassed with two cycles of freeze-pump-thaw and stored under protective conditions inside the glove box. LiCl (*Sigma-Aldrich*,

powder, ≥ 99.99 % trace metal basis), $MgCl_2$ (*Sigma-Aldrich*, "ultra dry", 99.999 %), $ZnCl_2$ (*Acros*, "extra pure", 99.999 %) and ZnI_2 (*Acros*, "extra pure", 99.999 %) were used as received and stored inside the glove box under exclusion of light. The solvents used in polymerization reactions were taken from a solvent purification system (*MBraun*, Germany) and stored under protective conditions over molecular sieves (3 Å). NHOs **1**, **3**, **4** and **5** were prepared according to literature, whereby identity was confirmed using ^{1}H and ^{13}C NMR analysis; full characterization is provided in the cited references.[1-4] Precursor salt **2'** was received following the general procedure for **1'**, using cyclization of a suitable diketone with (-)-citronellal, followed by methylation. For synthesis and characterization of NHO **2**, see below.

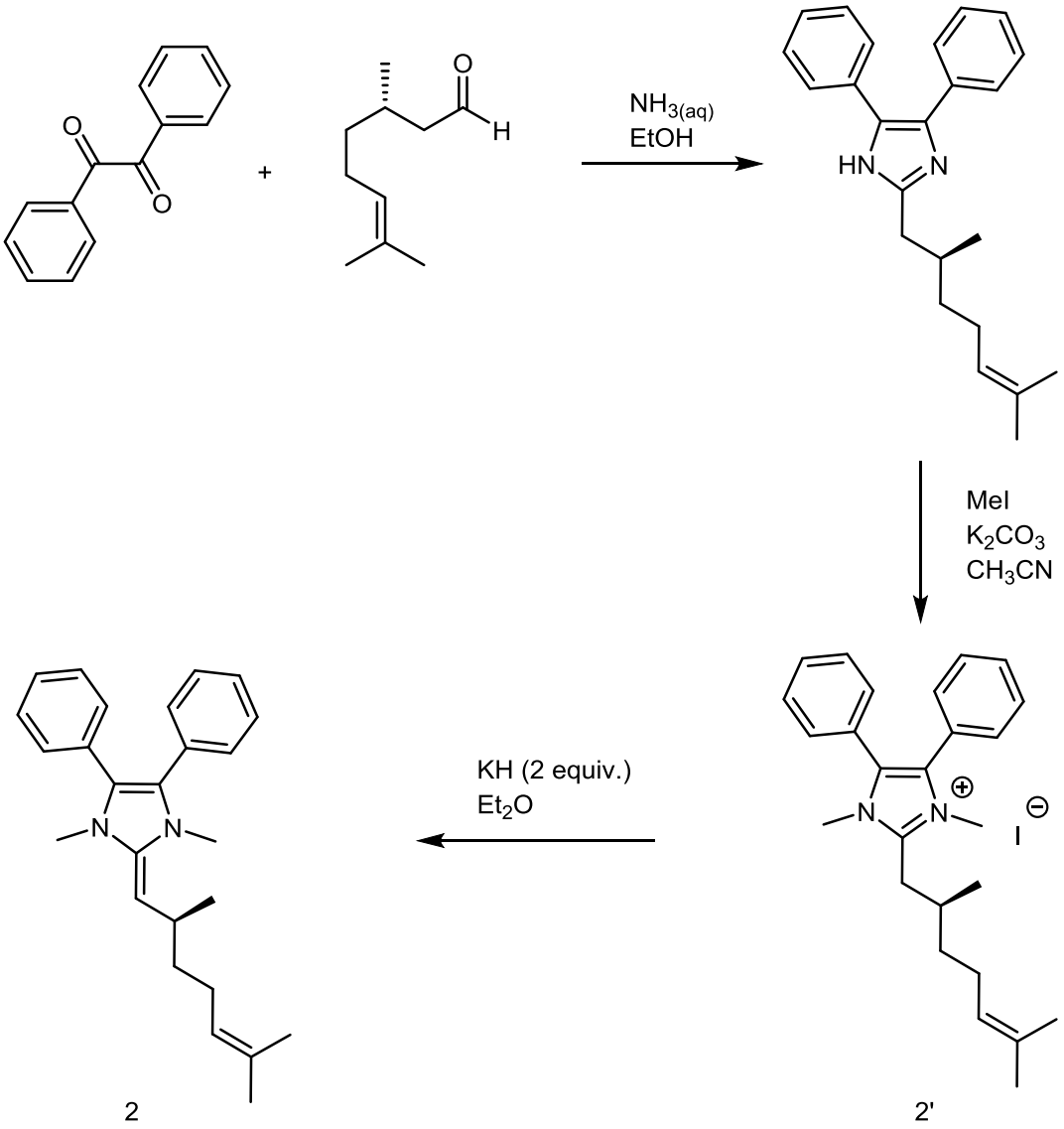

Figure S1. Schematic synthesis of NHO **2**.

Preparation of precursor salt 2'

Benzil (9.99 g; 47.5 mmol 0.9 eq), (*S*)-citronellal (9.45 g; 50mmol, 1 eq.) and aqueous ammonia solution (70 mL, 25%) were combined in ethanol (120 mL) and stirred for 3 h at 50 °C. The solution was allowed to cool down and was further stirred overnight at room temperature. The generated white precipitate was filtered off, washed with

EtOH and dried under reduced pressure. Yield: 2.36 g (6.85 mmol, 14%). The received white solid (2.0 g; 5.8 mmol, 1 eq.) was then combined with K_2CO_3 (0.48 g; 3.48 mmol, 0.6 eq.) in CH_3CN (20 mL) and stirred at room temperature. The reaction mixture was put in an ice bath and MeI (3.30 g; 23.2 mmol, 4 eq.) was added dropwise, followed by stirring at room temperature overnight. Subsequently, all volatiles were removed in vacuo, the residue was dissolved in dichloromethane and *n*-pentane was added. The DCM phase was isolated and dried in vacuo, yielding **2'** as yellowish foam. Yield: 2.91 g (5.8 mmol, 100%).

(*S*)-2-(2,6-dimethylhept-5-en-1-yl)-1,3-dimethyl-4,5-diphenyl-1H-imidazol-3-ium (2'): 2.91 g (solid, 14% yield). **^{1}H NMR** ($CDCl_3$): δ = 7.43 – 7.36 (*m*, 10H), 5.08 – 5.04 (*m*, 1H), 3.68 (*s*, 6H), 3.33 (*dq*, 1H), 2.20 – 1.97 (*m*, 3H), 1.66 (*dd*, 6H), 1.51 – 1.44 (*m*, 2H), 1.09 (*d*, 3H) ppm. **^{13}C-NMR** (CDCl3): 146.68, 132.85, 131.95,131.31, 130.23, 129.06, 125.50, 123.36, 123.32, 36.88, 34.08, 33.60, 32.32, 25.85, 25.37, 20.05, 18.02; **IR** (ATR, cm^{-1}): 3450 (m), 2960 (s), 2870 (s), 2790 (m), 1550 (s), 1480 (s), 1300 (w), 1050 (s), 770 (s), 690 (s); **HMRS (ESI)**: m/z calc. for $C_{26}H_{33}N_2^+$ = 373.2644, found: 373.2639.

Preparation of NHO 2

Precursor salt **2'** (2.4 g, 4.78 mmol, 1 eq.) was added under nitrogen flow to a Schlenk flask containing 40 mL of dry Et_2O and 383 mg of KH (9.56 mmol, 2eq.). Under exclusion of light, the suspension was stirred for two days at room temperature (H_2 allowed to escape via open Schlenk line). The product was then extracted from this suspension using dry *n*-pentane (inside the glove box). After removal of solvent, a yellow liquid (1.25g, 3.35 mmol, 70%) remained and was stored at -36 °C inside the glove box.

(*S*)-2-(2,6-dimethylhept-5-en-1-ylidene)-1,3-dimethyl-4,5-diphenyl-2,3-dihydro-1H-imidazole (4): 1.25 g (liquid, 70% yield). **^{1}H-NMR** (C_6D_6): δ = 7.35 – 7.05 (*m*, 10H), 5.59 – 5.55 (*m*, 1H), 3.29 (*d*, 1H), 3.15 (*s*, 3H), 3.00 – 2.93 (*m*, 1H), 2.78 (*s*, 3H), 2.55 – 2.51 (2H), 1.90 (*d*, 3H), 1.88 – 1.83 (*m*, 2H), 1.82 (*d*, 3H), 1.53 (*d*, 3H) ppm; **^{13}C-NMR** (C_6D_6): δ = 151.52, 131.45, 131.18, 130.46, 129.92, 128.73, 128.56, 128.42, 128.06, 125.92, 74.53, 41.01, 37.58, 31.99, 30.73, 26.83, 25.81, 25.05, 17.64 ppm; **HR-MS (ESI)**: m/z calc. for $C_{26}H_{32}N_2$ = 372.2565, found: 373.2638 $[NHO+H]^+$.

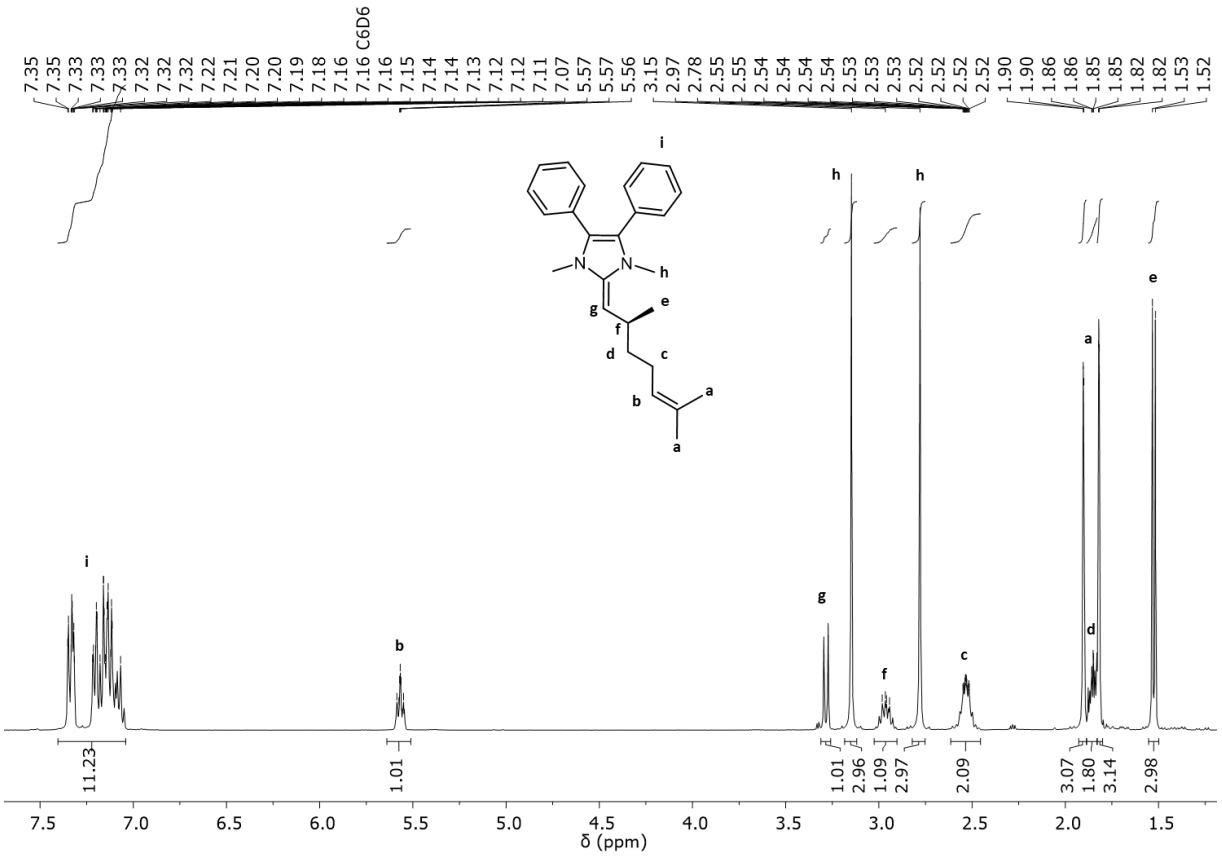

Figure S2. ^{1}H NMR analysis (C_6D_6, 400 MHz, 300 K) of NHO **2**.

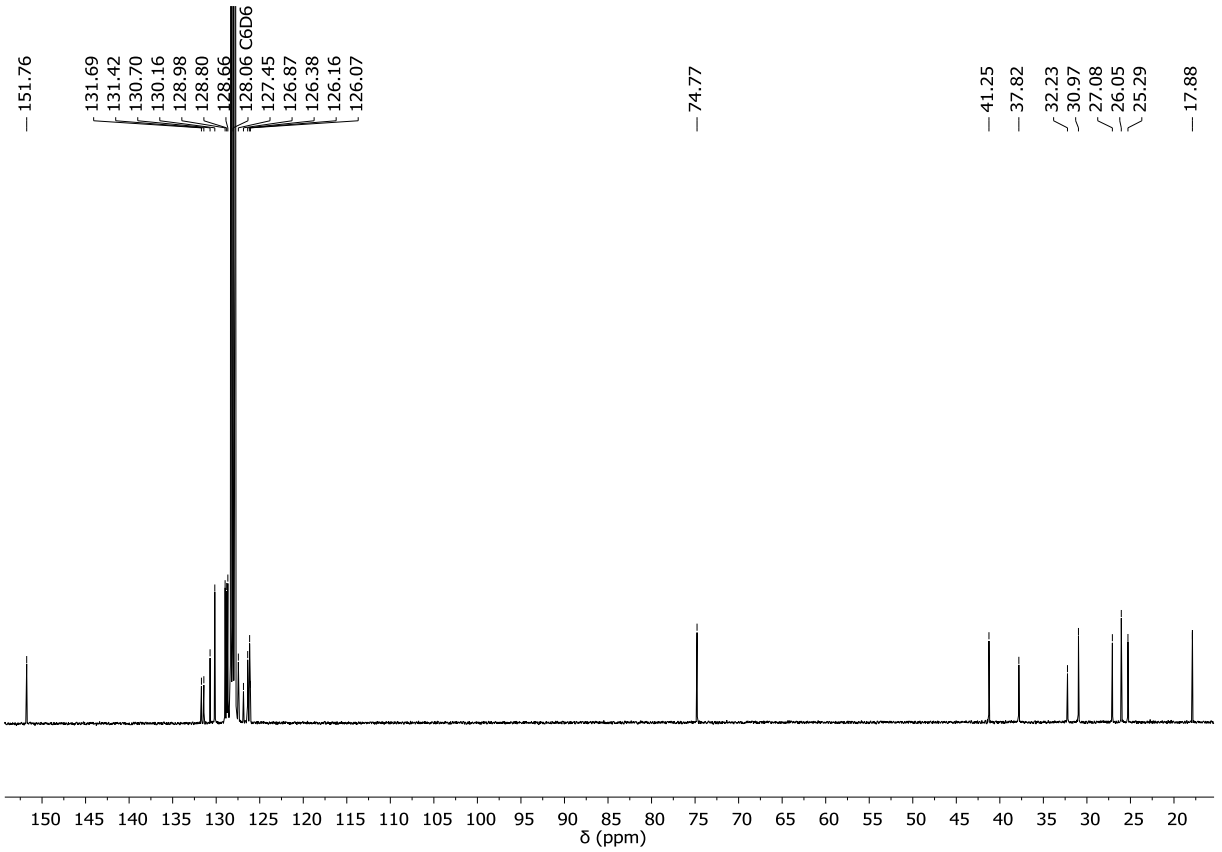

Figure S3. ^{13}C NMR analysis (C_6D_6, 100 MHz, 300 K) of NHO **2**.

General Polymerization Procedure

The polymerization setups were assembled and the reactions were carried out inside the glove box. For a typical polymerization, the Lewis acid (e.g., LiCl, 1.6 mg, 0.0375mmol, 3 eq.) was dissolved in dry THF (5mL) and combined with the monomer (*L*-LA, 900 mg, 6.25 mmol, 500 eq.). The organobase (e.g., NHO **1**, 2.1 mg, 0.0125 mmol, 1 eq.) was dissolved in THF (1 mL), the initiator was added (BnOH, 2.7 mg, 2.6 µL, 0.025 mmol, 2 eq.) and the two solutions were combined. The polymerization was quenched by addition of HCl in Et_2O and evaporation of the solvent. Conversion of *L*-LA was determined from ^{1}H NMR spectroscopy ($CDCl_3$), monitoring the methine region signals of the respective monomer (δ= 5.00 – 5.08 ppm) and the resulting polymer (δ= 5.10 – 5.25 ppm). Polydispersity ($Đ_M$) and molecular weight (M_n) were determined via GPC analysis ($CHCl_3$).

Characterization and Analysis

^{1}H, {^{1}H} and ^{13}C spectra were recorded on a *Bruker* Avance III 400 spectrometer. All chemical shifts are reported relative to the reference peak of deuterated chloroform (δ= 7.26 ppm for ^{1}H / δ= 77.16 ppm for ^{13}C) or deuterated benzene (δ= 7.16 ppm for ^{1}H / δ= 128.1 ppm for ^{13}C).

Molar masses and polydispersity of the different polymers were determined via gel permeation chromatography (GPC), employing a calibration versus polystyrene in the range of 800 g/mol - $2{\cdot}10^6$ g/mol. GPC measurements (40 °C) were carried out in $CHCl_3$ using an *Agilent* 1200 Series G1362A RI-detector. The seperation system was equipped with a *PSS* SDV 5 µm 8*50mm pre-column and three *PSS* SDV 100 000 Å 5µm 8*50mm columns. A flow rate of 1 ml/min and a sample concentration of 2 mg/ml were applied (100 µL injection).

MALDI-ToF (matrix-assisted laser desorption ionization-time of flight) mass spectrometry measurements were conducted on a *Bruker* Autoflex III (337nm, reflector mode). The samples were prepared by mixing matrix solution (2,5-dihydroxybenzoic acid, 5 mg/mL in THF), PLA solution (5 mg/mL in THF), and sodium triflouromethanesulfonate solution used as cationization agent (0.1 M in 90% acetone/water = 9:1) with a ratio of 2:1:2. For calibration, a poly(styrene) standard was employed.

For Differential Scanning Calorimetry (DSC), a Perkin Elmer DSC 4000 was used (scanning rate 10 K/min, 20 mL nitrogen flow, temperature range -20 °C to 250 °C). Thermograms were analyzed using the second heating/cooling cycle.

Calculation of P_r Values of Polymers Obtained by ROP of *rac*-LA

For the calculation of P_r, homodecoupled ^{1}H NMR spectra were recorded and the areas at δ = 5.24 - 5.19 ppm (*rmr* and *rmm*/*mmr* = *I1*) and at δ = 5.19 - 5.13 ppm (*mmr/rmm*, *mmm* and *mrm* = *I2*) were integrated and the values inserted according to $P_m = 1 - 2 \cdot I_1/(I_1+I_2)$.[6] To countercheck these results, deconvolution using NMR software (Mestre) and Bernoullian statistics, assuming chain end-control (CEC), were applied. Both methods delivered similar results (see Figure S4 for an example).

Table S1. Tetrad probabilities of CEC mechanisms based on Bernoullian statistics.[5]

tetrad	Probability of CEC (Bernoullian)
mmm	$P_m^2+0.5\ P_mP_r$
mmr	$0.5\ P_mP_r$
rmm	$0.5\ P_mP_r$
rmr	$0.5\ P_r^2$
mrm	$0.5\ (P_m^2+ P_mP_r)$

tetrad	ppm	ratio
rmr	5.22	0,386241307
rmm/mmr	5.20	0,059345588
mmr/rmm	5.17	0,011059026
mmm	5.16 – 5.15	0,07101295
mrm	5.14	0,472341129

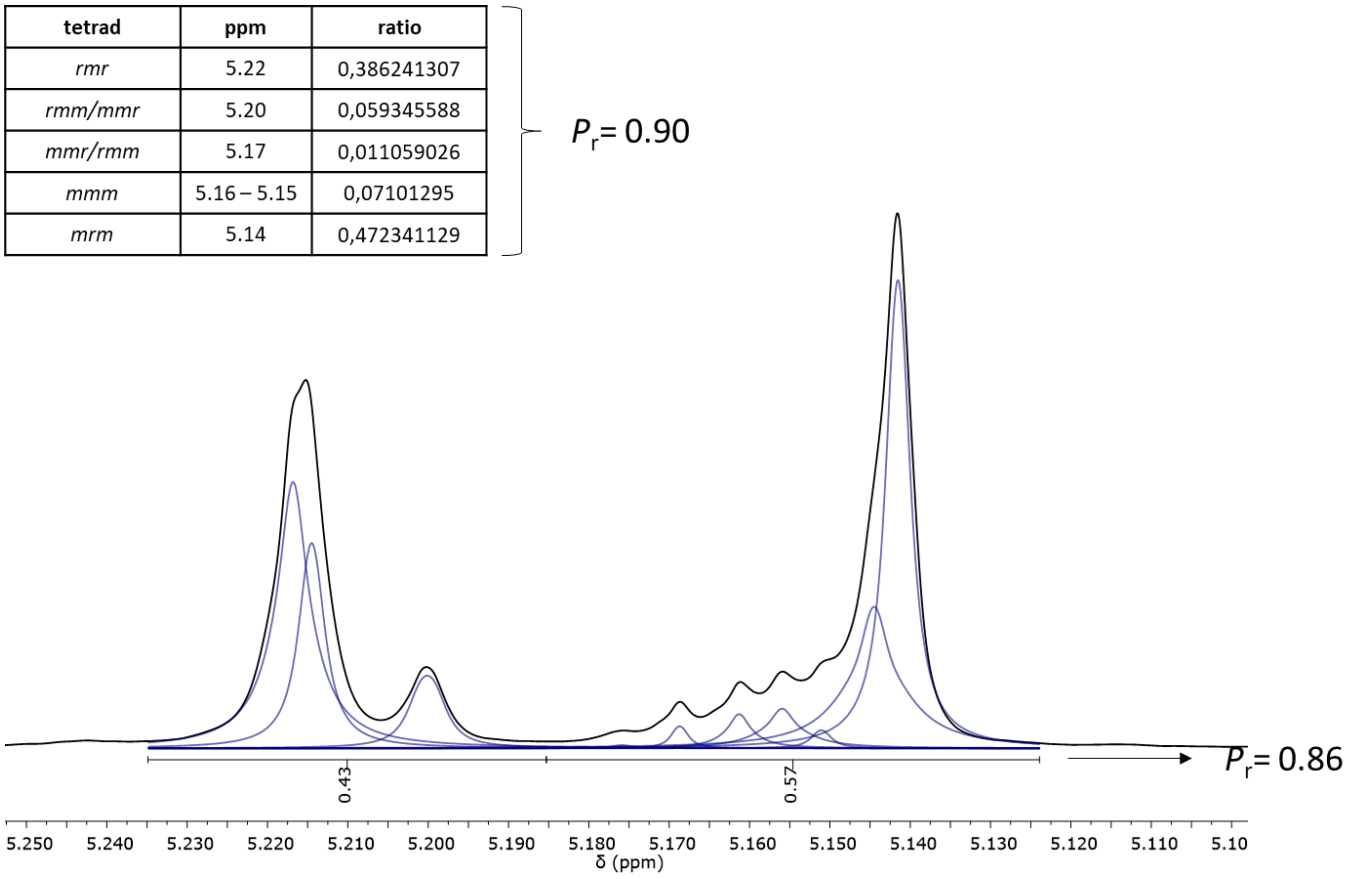

Figure S4. Homonuclear decoupled ^{1}H {^{1}H} NMR spectrum (400 MHz, $CDCl_3$) of the methine region of PLA obtained by the action of **3**/$ZnCl_2$ (Table S2, entry 31, zwitterionic).

Tabular Data

Table S2. Reactions using NHO **1**-**5**/BnOH/MX_n/*L*-LA in THF (1 M).

#	NHO	MX_n	Initiator	NHO : BnOH : MX_n: M	c(M) in THF	t [min]	conv. [%][a)]	Mn [kg/mol][b)]	$Đ_M$[b)]
1	1	LiCl	BnOH	1:2:3:500	1 M	15	96	53	1.49
2	2	LiCl	BnOH	1:2:3:500	1 M	15	98	50	1.52
3	3	LiCl	BnOH	1:2:3:500	1 M	15	95	48	1.54
4	4	LiCl	BnOH	1:2:3:500	1 M	15	97	51	1.53
5	5	LiCl	BnOH	1:2:3:500	1 M	15	96	54	1.47
6	1	$MgCl_2$	BnOH	1:2:3:500	1 M	360	18	7.4	1.06
7	2	$MgCl_2$	BnOH	1:2:3:500	1 M	360	20	8.2	1.06
8	3	$MgCl_2$	BnOH	1:2:3:500	1 M	360	11	3.3	1.10
9	4	$MgCl_2$	BnOH	1:2:3:500	1 M	360	19	9.0	1.05
10	5	$MgCl_2$	BnOH	1:2:3:500	1 M	360	13	4.7	1.14
11	1	$ZnCl_2$	BnOH	1:2:3:500	1 M	360	19	5.4	1.10
12	2	$ZnCl_2$	BnOH	1:2:3:500	1 M	360	17	6.3	1.07
13	3	$ZnCl_2$	BnOH	1:2:3:500	1 M	360	23	4.3	1.08
14	4	$ZnCl_2$	BnOH	1:2:3:500	1 M	360	21	12.7	1.04
15	5	$ZnCl_2$	BnOH	1:2:3:500	1 M	360	14	5.6	1.13
16	1	LiCl	-	1:0:3:500	1 M	15	84	63	1.59
17	2	LiCl	-	1:0:3:500	1 M	15	81	72	1.40
18	3	LiCl	-	1:0:3:500	1 M	15	83	86	1.50
19	4	LiCl	-	1:0:3:500	1 M	15	78	81	1.57
20	5	LiCl	-	1:0:3:500	1 M	15	81	71	1.47
21	1	$MgCl_2$	-	1:0:3:500	1 M	360	19	21	1.03
22	2	$MgCl_2$	-	1:0:3:500	1 M	360	12	25	1.03
23	3	$MgCl_2$	-	1:0:3:500	1 M	360	12	23	1.04
24	4	$MgCl_2$	-	1:0:3:500	1 M	360	11	21	1.05
25	5	$MgCl_2$	-	1:0:3:500	1 M	360	6	8.0	1.37
26	1	$ZnCl_2$	-	1:0:3:500	1 M	360	21	23	1.04
27	2	$ZnCl_2$	-	1:0:3:500	1 M	360	12	30	1.05
28	3	$ZnCl_2$	-	1:0:3:500	1 M	360	13	26	1.22
29	4	$ZnCl_2$	-	1:0:3:500	1 M	360	16	34	1.03
30	5	$ZnCl_2$	-	1:0:3:500	1 M	360	12	4.0	1.38
31	3	LiCl	BnOH	1:2:3:1000	2 M	2	92	70	1.54
32	3	LiCl		1:0:3:1000	2 M	2	60	62	1.69

a) Determined by ^{1}H NMR analysis (400 MHz, $CDCl_3$); b) determined via GPC ($CHCl_3$)

Table S3. Reactions using NHO **1**-**5**/BnOH/MX_n/*rac*-LA in THF (0.5 M).

#	NHO	MX_n	Initiator	NHO/-OH /MX_n/M	c(M) in THF	t [min]	conv.[%][a)]	Mn [kg/mol][b)]	$Đ_M$[b)]	P_r[c)]
1	1	LiCl	BnOH	1:2:3:250	0.5 M	15	94	15	1.38	0.56
2	2	LiCl	BnOH	1:2:3:250	0.5 M	15	98	14	1.38	0.56
3	3	LiCl	BnOH	1:2:3:250	0.5 M	15	>99	15	1.34	0.58
4	4	LiCl	BnOH	1:2:3:250	0.5 M	15	>99	16	1.37	0.56
5	5	LiCl	BnOH	1:2:3:250	0.5 M	15	94	2.8	4.29	0.56
6	3	$MgCl_2$	BnOH	1:2:3:250	0.5 M	360		3.1	1.15	0.62
7	5	$MgCl_2$	BnOH	1:2:3:250	0.5 M	360	27	2.7	1.16	0.62
8	1	$ZnCl_2$	BnOH	1:2:3:250	0.5 M	360	41	6.3	1.07	0.92
9	3	$ZnCl_2$	BnOH	1:2:3:250	0.5 M	360	60	11	1.07	0.72
10	4	$ZnCl_2$	BnOH	1:2:3:250	0.5 M	360	51	9.3	1.06	0.90
11	5	$ZnCl_2$	BnOH	1:2:3:250	0.5 M	360	37	6.6	1.11	0.80
12	1	LiCl	-	1:0:3:250	0.5 M	15	97	3.4	8.11	0.74
13	2	LiCl	-	1:0:3:250	0.5 M	15	97	3.4	8.83	0.74
14	3	LiCl	-	1:0:3:250	0.5 M	15	96	3.0	13.6	0.74
15	4	LiCl	-	1:0:3:250	0.5 M	15	95	4.7	13.2	0.70
16	5	LiCl	-	1:0:3:250	0.5 M	15	93	3.4	7.01	0.72
17	1	$ZnCl_2$	-	1:0:3:250	0.5 M	360	35	3.2	1.11	0.86
18	4	$ZnCl_2$	-	1:0:3:250	0.5 M	360	35	9.1	2.04	0.84
19	5	$ZnCl_2$	-	1:0:3:250	0.5 M	360	23	10	1.20	0.86
20	3	LiI	BnOH	1:3:2:250	0.5 M	0.25	93	2.2	4.59	0.56
21	3	LiI		1:3:0:250	0.5 M	0.25	75	3.3	5.22	0.74
22	5	-		1:0:0:250	0.5 M	6	29	4.7	1.29	0,54
23	3	$MgCl_2$	BnOH	1:3:2:250	1 M	24	33	56	1.09	0.58
24	3	$MgCl_2$		1:2:0:250	1 M	24	47	36	1.07	0.74
25	3	$ZnCl_2$	BnOH	1:3:2:250	1 M	24	90	12	1.11	0.86
26	1	$ZnCl_2$		1:3:0:250	1 M	24	80	37	1.69	0.60
27	3	ZnI_2		1:3:0:250	1 M	24	80	73	1.26	0.98
28	2	$MgCl_2$	BnOH	1:3:2:250	0.5 M	24	51	10	1.11	0.56
29	2	$MgCl_2$		1:0:2:250	0.5 M	24	42	34	1.13	0.56
30	2	$ZnCl_2$	BnOH	1:3:2:250	0.5 M	24	73	15	1.14	0.82
31	2	$ZnCl_2$		1:3:0:250	0.5 M	24	75	74	1.29	0.86
32	2	-	BnOH	1:0:2:250	0.5 M	24	77	7.8	1.25	0.48
33	4	-	BnOH	1:0:2:250	0.5 M	24	79	13	1.28	0.48

a) determined *via* ^{1}H NMR; b) according to GPC ($CHCl_3$); c) determined according to Schaper; d) $[M]_0$ = 1.0 mol/L.

Maldi-ToF MS Analysis

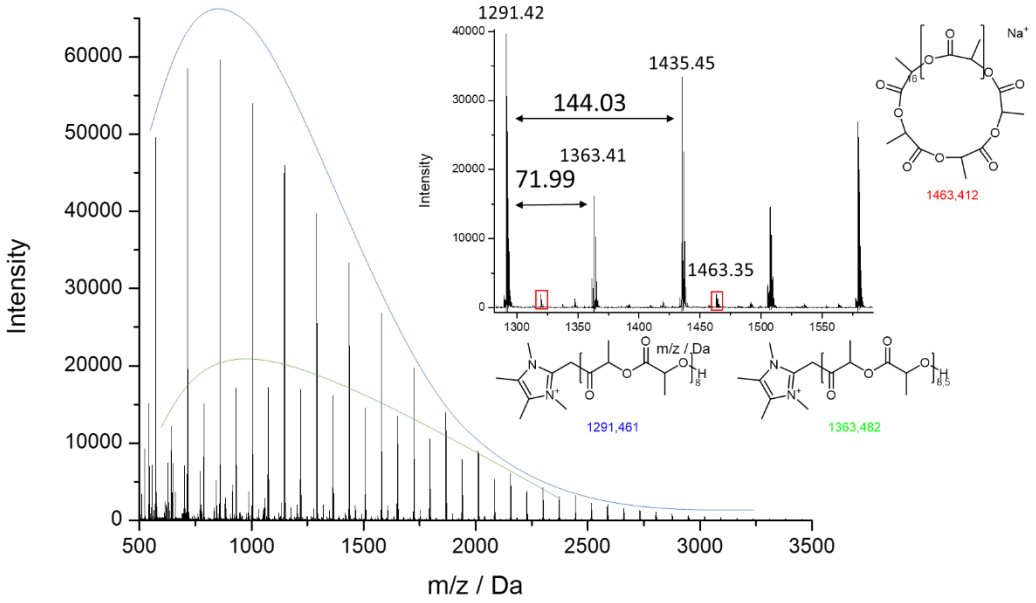

Figure S5. MALDI-ToF analysis of PLA (*L*-LA) prepared by the action of **5**/$ZnCl_2$.

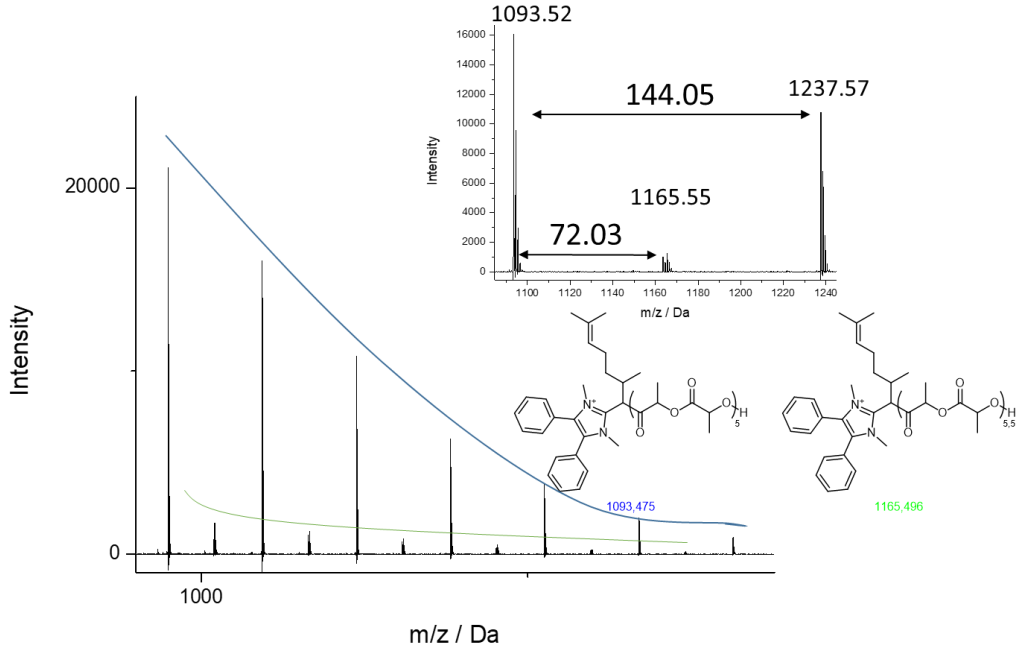

Figure S6. MALDI-ToF analysis of PLA (*L*-LA) prepared by the action of **2**/$ZnCl_2$.

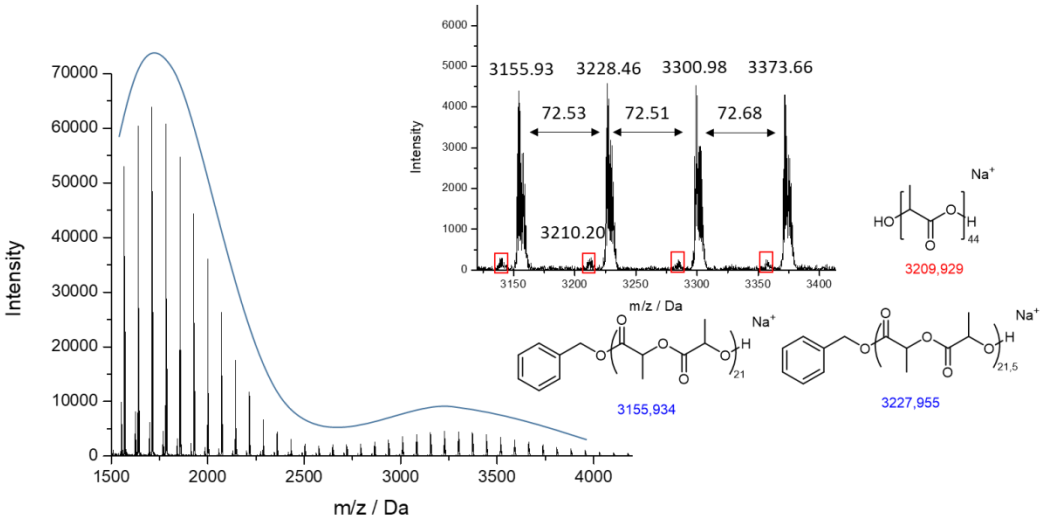

Figure S7. MALDI-ToF MS analysis of PLA (*L*-LA) prepared by the action of **1**/LiCl and BnOH, cationized by sodium.

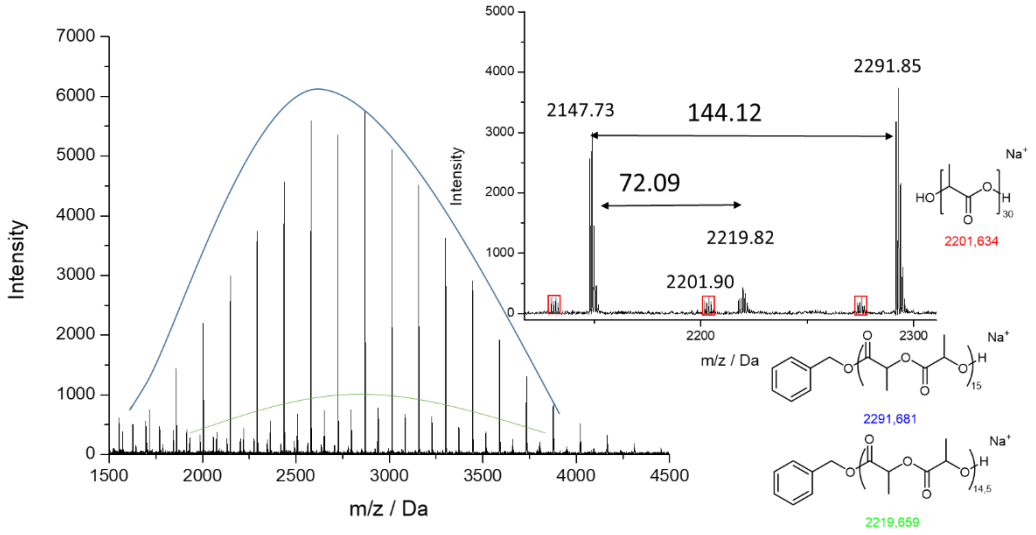

Figure S8. MALDI-ToF analysis of PLA (*L*-LA) prepared by the action of **1**/$ZnCl_2$ and BnOH, cationized by sodium.

Kinetic Data

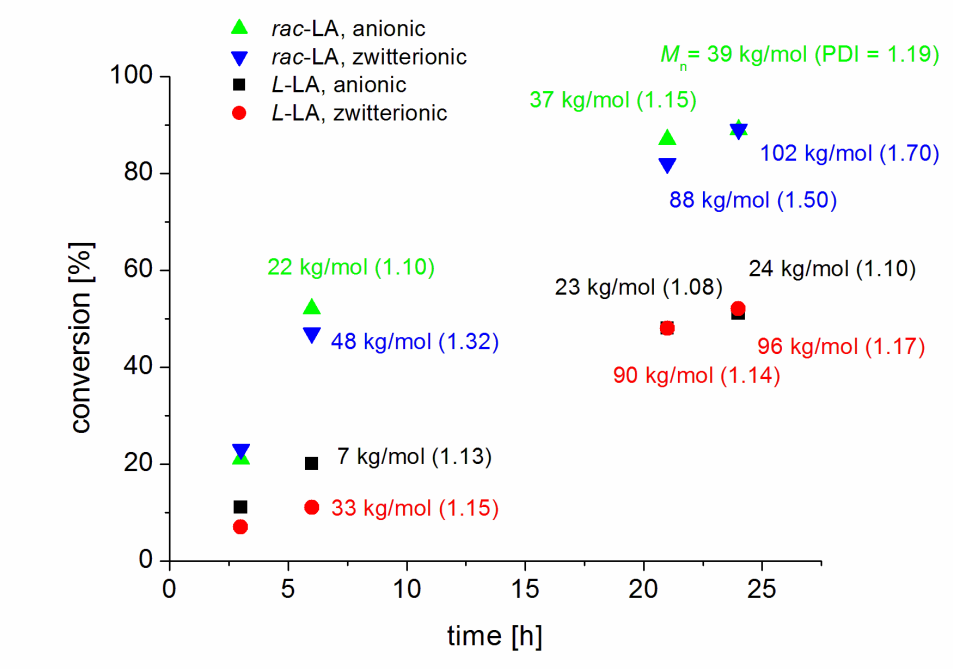

Figure S9. Kinetic plots of the anionic and zwitterionic ROP of *L*-LA and *rac*-LA by **3**/$ZnCl_2$ in THF at RT, 0.5 M. [NHO]:[BnOH]:[$ZnCl_2$]:[LA] = 1:2:3:500 or 1:0:3:500. Molar mass (M_n) and polydispersity ($Đ_M$) are also given, showing the expected chain growth and a broadening of molar mass distribution at higher conversion, mirroring intensified transesterification under monomer-starved conditions.

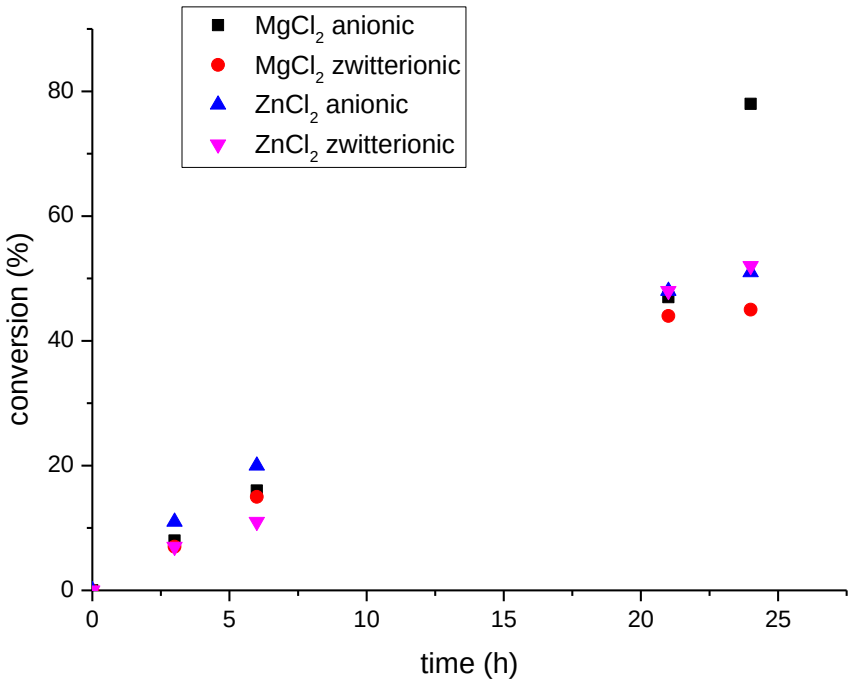

Figure S10. Conversion vs. time for the polymerization of *L*-LA, applying NHO **3** with different Lewis acids along zwitterionic or anionic polymerization pathways. *L*-LA , **3**/$MgCl_2$ in THF at RT, 0.5 M. [NHO]/[BnOH]/[$MgCl_2$]/[*L*-LA] = 1:2:3:500 or 1:0:3:500.

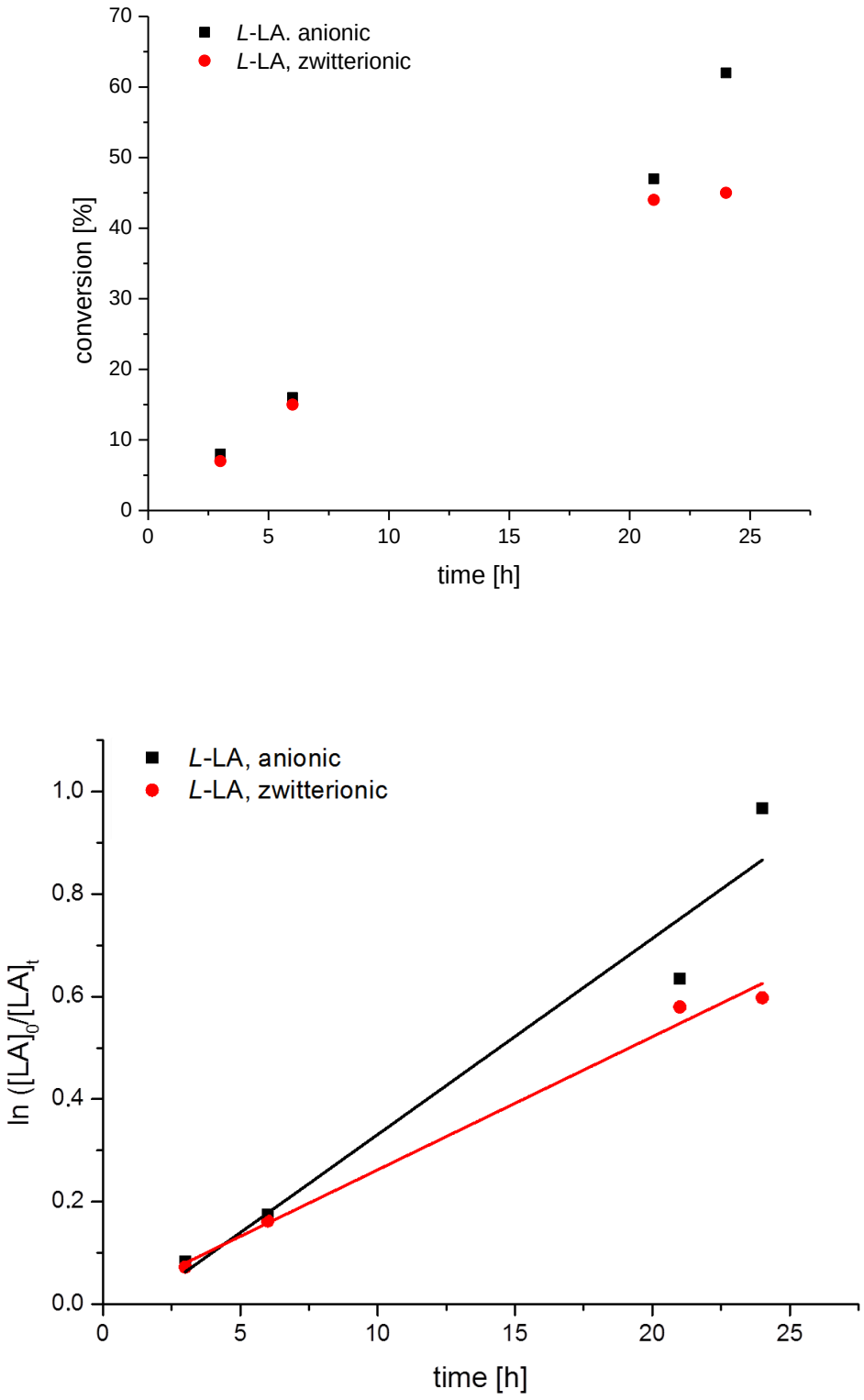

Figure S11. Anionic and zwitterionic ROP of *L*-LA , **3**/$MgCl_2$ in THF at RT, 0.5 M. [NHO]/[BnOH]/[$MgCl_2$]/[*L*-LA] = 1:2:3:500 or 1:0:3:500.

Homodecoupled ^{1}H $\{^{1}H\}$ NMR

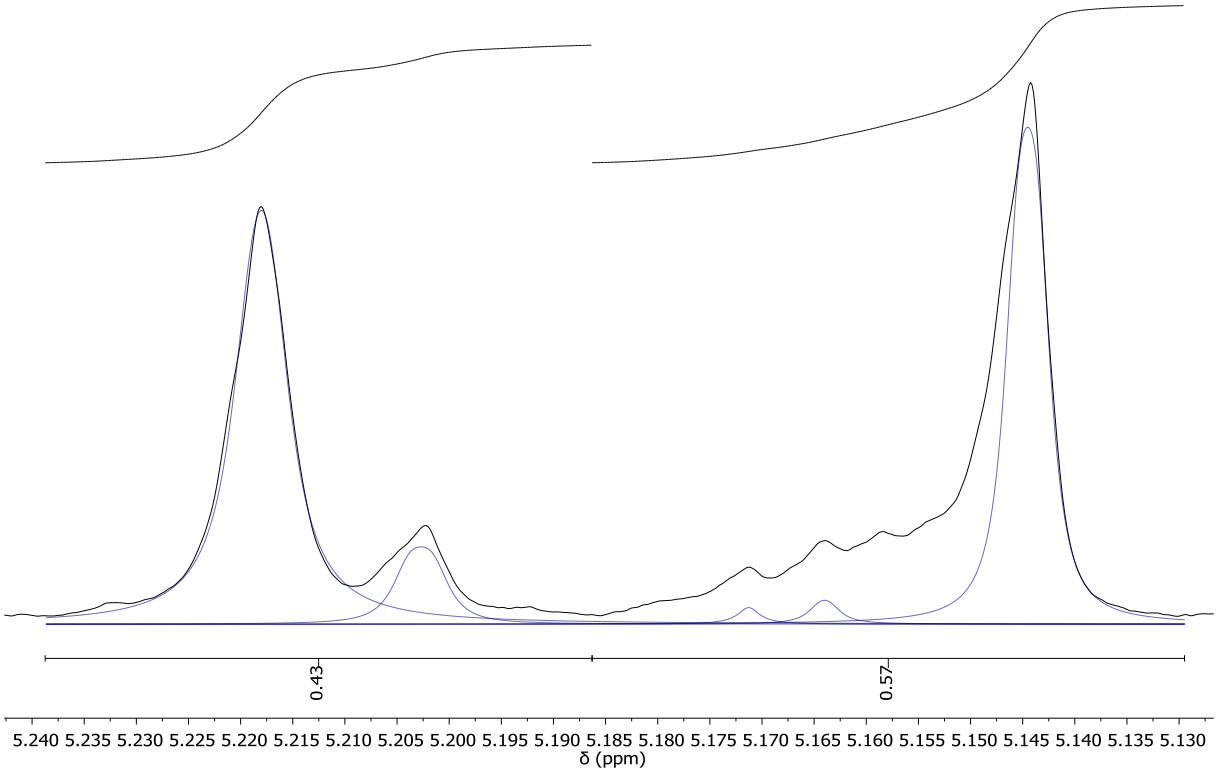

Figure S12. Homonuclear decoupled ^{1}H $\{^{1}H\}$ NMR spectrum (400 MHz, $CDCl_3$) of the methine region of PLA obtained by the action of **5**/$ZnCl_2$ (Table S2, entry 19, zwitterionic).

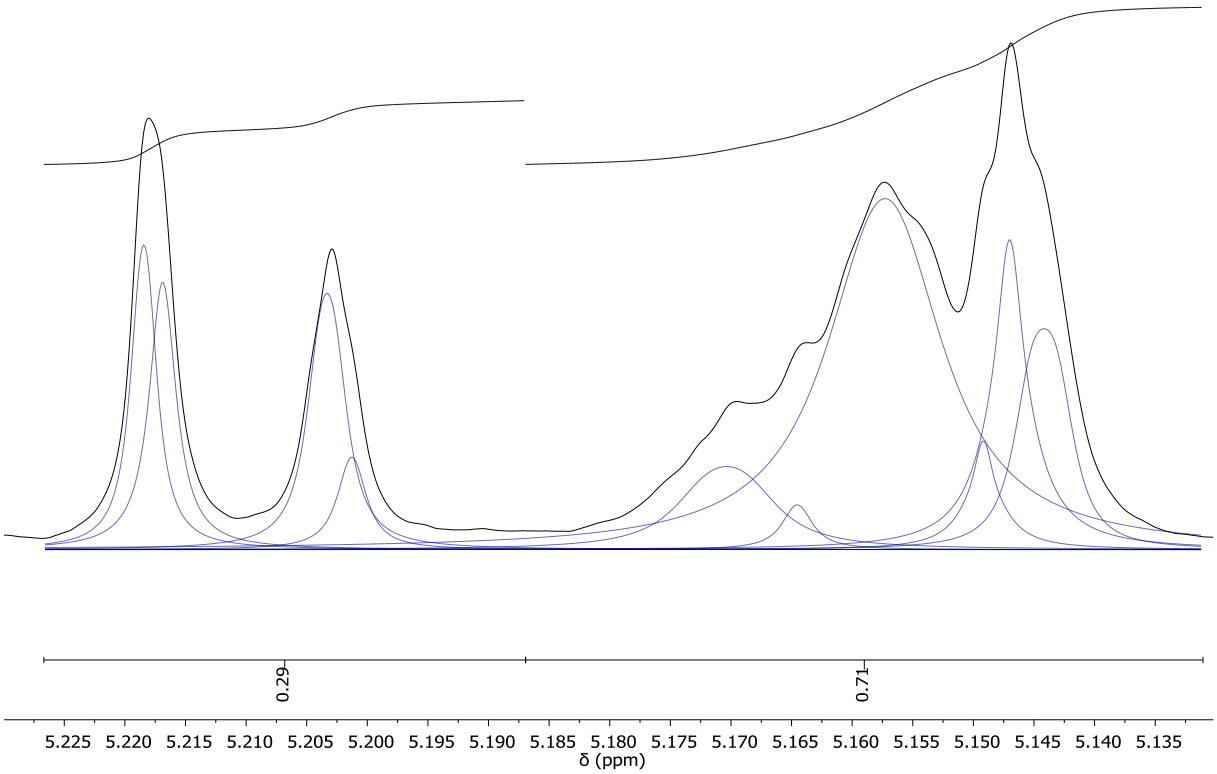

Figure S13. Homonuclear decoupled ^{1}H {^{1}H} NMR spectrum (400 MHz, $CDCl_3$) of the methine region of PLA obtained by the action of **3**/$MgCl_2$ (Table 2, entry 7, anionic).

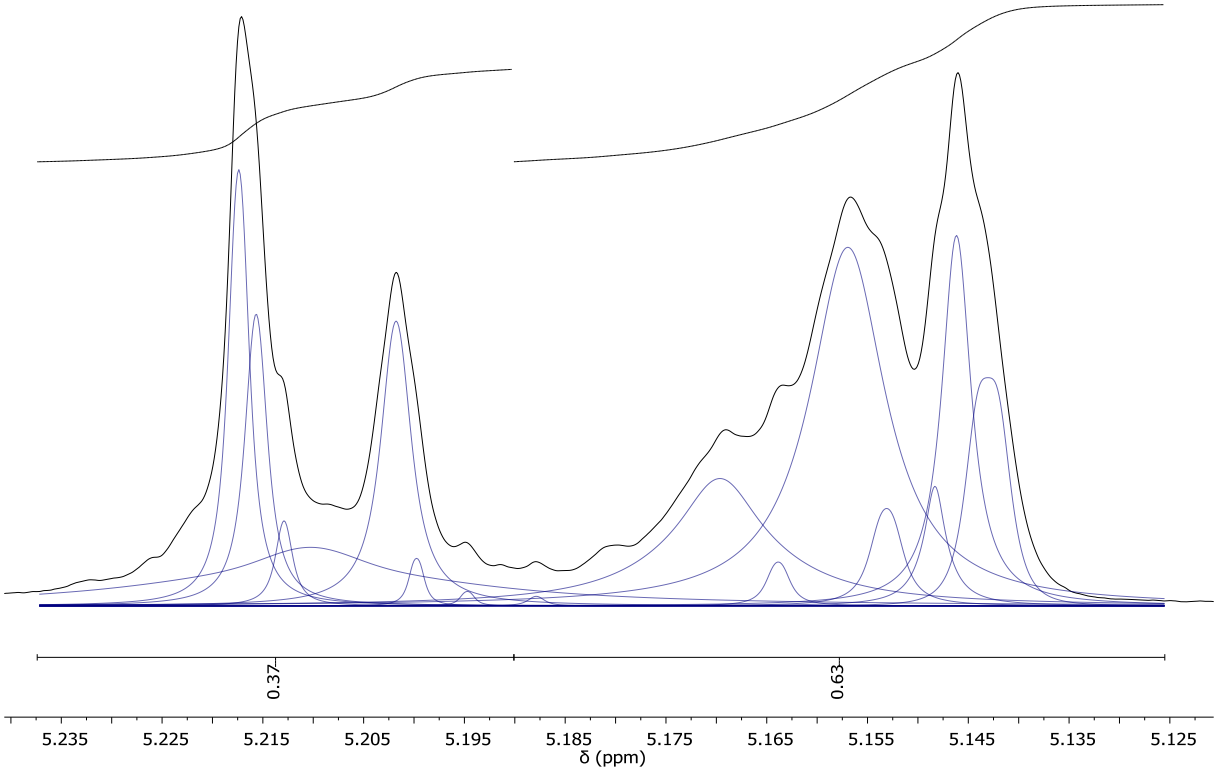

Figure S14. Homonuclear decoupled ^{1}H {^{1}H} NMR spectrum (400 MHz, $CDCl_3$) of the methine region of PLA obtained by the action of **3**/$MgCl_2$ (Table 2, entry 8, zwitterionic).

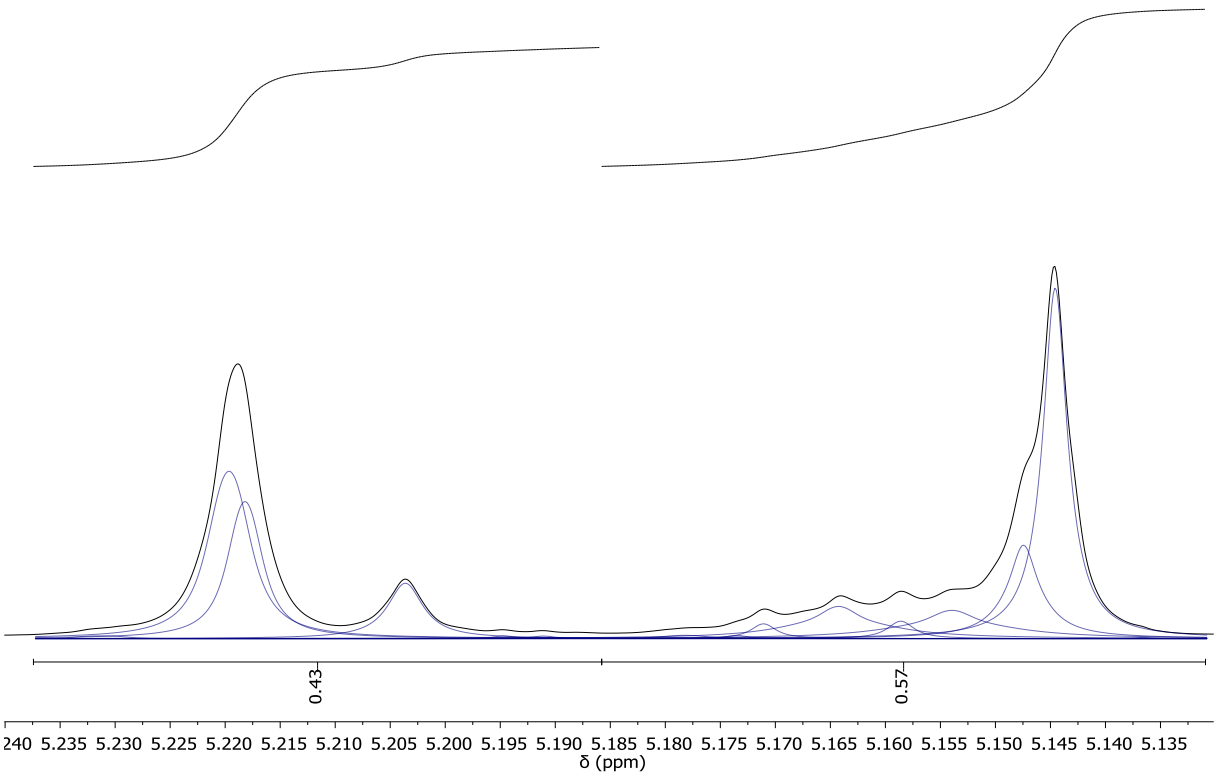

Figure S15. Homonuclear decoupled ^{1}H $\{^{1}H\}$ NMR spectrum (400 MHz, $CDCl_3$) of the methine region of PLA obtained by the action of **3**/$ZnCl_2$ (Table 2, entry 10, anionic).

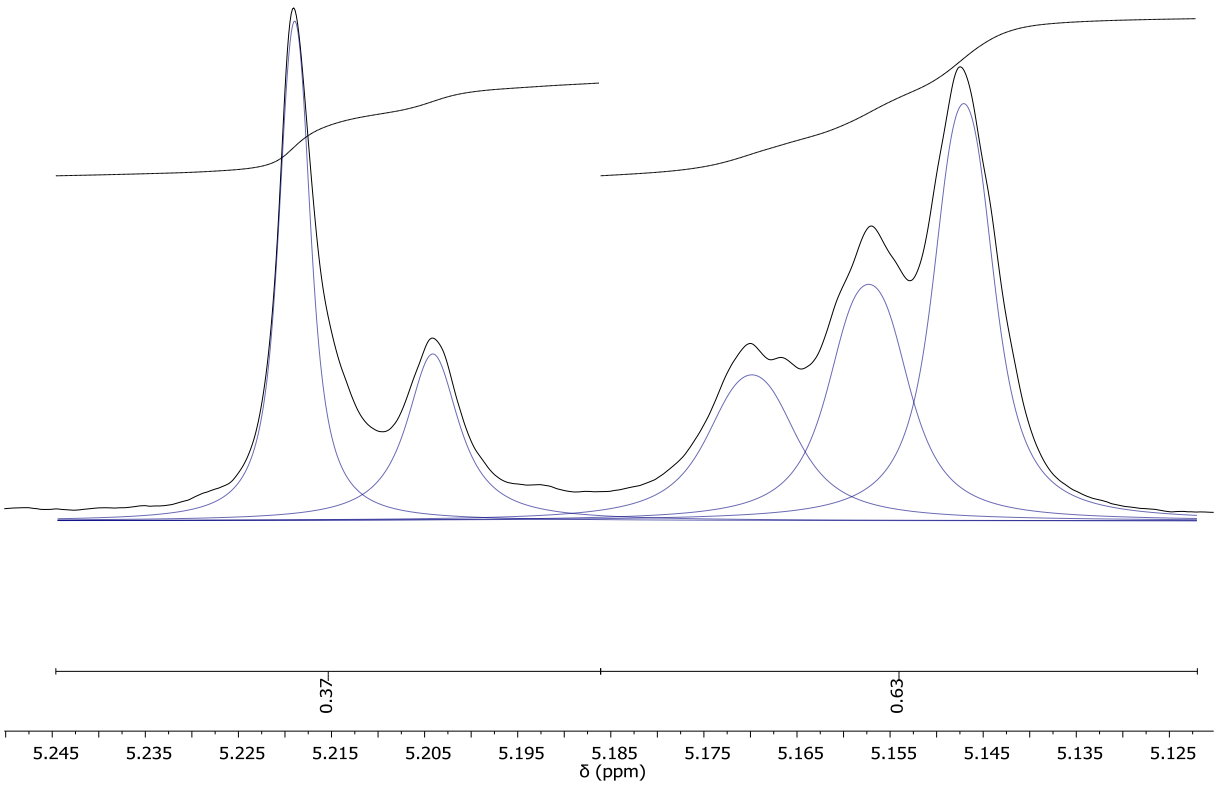

Figure S16. Homonuclear decoupled ^{1}H $\{^{1}H\}$ NMR spectrum (400 MHz, $CDCl_3$) of the methine region of PLA obtained by the action of **3**/LiI (Table S2, entry 21, zwitterionic).

Differential Scanning Calorimetry

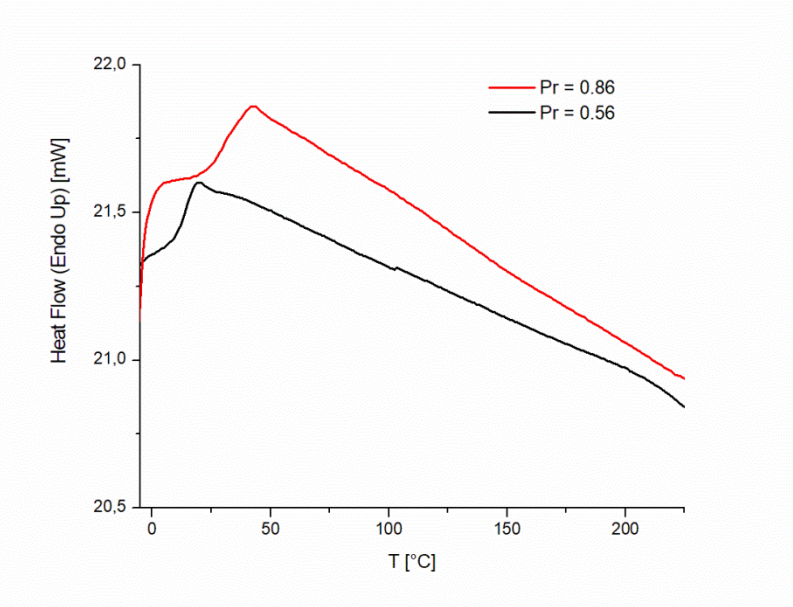

Figure S17. Thermograms of PLA samples (DSC, heating and cooling rate of 10 K/min, second cycle) with different degree of heterotacticity. For reaction conditions, see Table S3, entry 1, and Table S3, entry 31.

References

[1] S. Naumann and D. Wang, *Macromolecules*, 2016, **49**, 8869–8878.

[2] M. H. U. Gruseck, *Chem. Ber.*, 1987, **120**, 2053–2064.

[3] S. Naumann, A. W. Thomas, A. P. Dove, *Angew. Chem. Int. Ed.*, 2015, **54**, 9550–9554.

[4] a) H. Quast, M. Ach, M. K. Kindermann, P. Rademacher, M. Schindler, *Chem. Ber.*, 1993, **126**, 503–516; b) S. Kronig, P. G. Jones, M. Tamm, *Eur. J. Inorg. Chem.*, 2013, **13**, 2301– 2314.

[5] B. M. Chamberlain, M. Cheng, D. R. Moore, T. M. Ovitt, E. B. Lobkovsky, G. W. Coates, *J. Am. Chem. Soc.*, 2001, **123**, 3229-3238.

[6] P. Daneshmand, J. L. Jiménez-Santiago, M. Aragon-Alberti, F. Schaper, *Organometallics*, 2018, **37**, 1751-1759.